

A Distraction Score for Watermarks

Aurelia Guy
Google

liaguy@google.com

Sema Berkiten
Google

berkiten@google.com

Abstract

In this work we propose a novel technique to quantify how distracting watermarks are on an image. We begin with watermark detection using a two-tower CNN model composed of a binary classification task and a semantic segmentation prediction. With this model, we demonstrate significant improvement in image precision while maintaining per-pixel accuracy, especially for our real-world dataset with sparse positive examples. We fit a nonlinear function to represent detected watermarks by a single score correlated with human perception based on their size, location, and visual obstructiveness. Finally, we validate our method in an image ranking setup, which is the main application of our watermark scoring algorithm.

1. Introduction

Watermarking images is a common practice for both businesses and individuals to mark ownership. Oftentimes, the watermark is small and can be ignored, only taking up a small portion of the image and not taking away from the overall image quality. However there is a subset of watermarks that greatly impact visual quality. For these images, the visual quality is greatly decreased by their watermarks. In this work we aim to infer an image score that encodes its watermarks' perceptual impact. One of the major motivation for such a score is to demote images based on how distracting their watermarks are for an image ranking task such as for image ranking in Google Maps. Our objective is to score images with high precision for the broad watermark class, which includes watermarks that range from mostly transparent to fully opaque, as well as watermarks of arbitrary *shapes, texts, and patterns*.

Our work is performed on a proprietary dataset of 200k annotated images, taken by individuals or businesses. As the majority of images in our full database do not contain watermarks, we additionally consider the performance of our model in terms of real world data, which we estimate to contain less than 10% watermarked images by randomly sampling our database of billions of images.

DeepLab. In this work, we formulate our problem of detecting watermarks as a combination of binary image classification, used to improve our precision, and a semantic image segmentation task. To train our model, we use a variation of the DeepLab architecture [7]. The DeepLab framework implements atrous convolution with an encoder-decoder structure [8, 9] to segment objects at multiple scales [6, 7]. We utilize a variation of this model with the final Fully Connected CRF layer replaced by likelihood thresholding. The class likelihood scores for all scales are merged and thresholded to obtain the segmentation labels.

In this work, our contribution is twofold:

- A two-tower CNN architecture to train a segmentation model detecting watermarks with high reliability as shown in Figure 1;
- A scoring function to convert detected watermarks into a single score which represents human response to the watermarks' obstructiveness.

2. Related Work

Text Detector. An alternative approach for watermark detection is a text detector, as many watermarks contain text. In section 4.5, we compare the inference results for Google Cloud API's text detector [2] to our trained DeepLab-based model. We demonstrate that the frequency of false positives in the results from a text detector model makes it unsuitable for our watermark detection task.

Watermark Removal. Another interesting and related problem to our task is watermark removal to recover the original image. Dekel et al. [12] demonstrate this approach with transparent watermarks of limited, predetermined types. This work leverages the consistent manner through which watermarks are added to images, as similar versions of logos are added to millions of images on the web. The removal problem is treated as a multi-image matting problem [16, 20] to separate the images into foreground and background, where the image structures of the common watermarks in a collection of images are utilized to detect

Hybrid Model

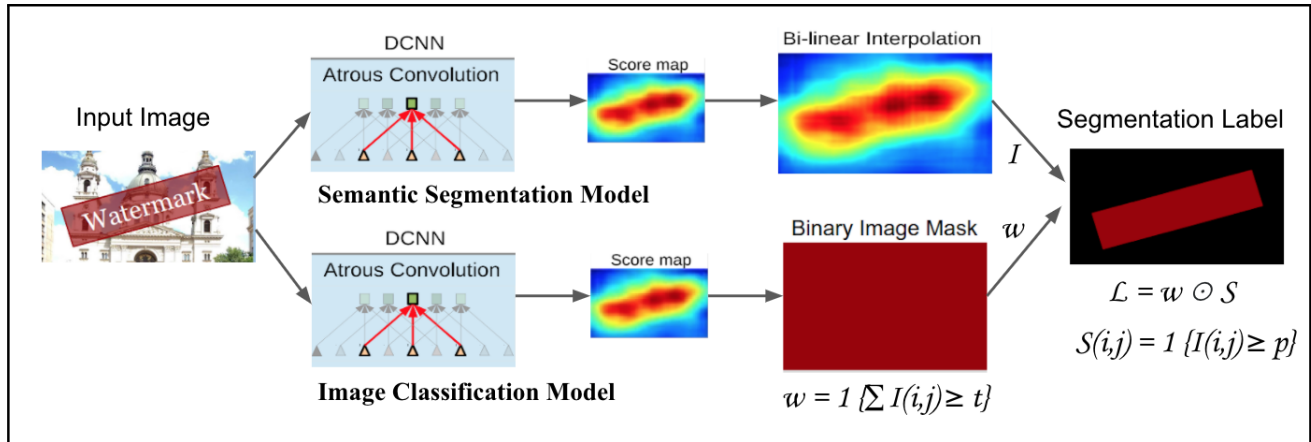


Figure 1: Diagram of the proposed hybrid model. A watermarked image is input to the image segmentation and classification models based on the DeepLab architecture [7]. binary image mask (w) is a black or white image based on the number of pixels is below or above (t). The final segmentation label (L) is obtained by taking inner product of the binary image mask w and segmentation map S where S is a binary image obtained by thresholding (p) score map I .

and remove the watermarked regions. This work generalizes to positional variations and subtle geometric and color variations only. Alternative watermark removal techniques include the use of image inpainting [4, 14] and Independent Component Analysis [17] to separate the watermark from the image. Braudaway et al. [5] introduced a digital watermarking technique for applying a watermark over an image while not obstructing any of the image detail. Similarly, Kankanhalli et al. [15] developed a method to construct pleasant and unobtrusive watermarked images based on the content of image. Watermark removal has also been demonstrated by Belmont [3] who adds a mask to an image and trains the network to find where the mask was overlaid. This architecture does not generalize well to watermarks that differ significantly from the generated watermark, however, and requires that the watermark is overlaid in an additive fashion. Related to removing watermarks in images is watermark removal in videos, which relies on temporal consistency [11, 21, 22]. In our work, we investigate detecting watermarks of varying image structures and do not restrict our model to synthetic or repeating data.

Mask R-CNN. Similar approaches to our image segmentation task are Mask R-CNN and DeepMask, which construct masks for image patches used for object proposals [13, 18]. In addition, Pinheiro et al. [19] introduces a feed-forward architecture which outputs a coarse mask encoding in the feed-forward pass. Dai et al. [10] uses a cascading architecture with three networks, including a mask estimation. However, the networks introduced in these works share convolutional features during training. We train our mask network separately on a dataset with negative examples and prioritize per pixel precision over accuracy. Our mask and segmentation networks are then combined after

training. As a result, our proposed network improves ranking accuracy for data with few positive examples.

3. Method

In the initial training of our DeepLab model for image segmentation, we observed a high frequency of image false positives. Images that contained signs, billboards, menus, and other text or logos that resembled watermarks were falsely predicted to contain watermarks. In order to reduce the frequency of these predictions, we developed a model that favored precision over recall, increasing the likelihood threshold for a watermark pixel and adding negative examples to our training dataset.

A limitation of our strict model is a decrease in per pixel recall for images that contained watermarks. We observe that by penalizing watermark pixel loss for images that only contained 6% watermark pixels, we are biasing our model towards negative predictions. DeepLab’s semantic segmentation model calculates the total loss at each iteration as the sum of the loss of each class. Since the non-watermark class comprises 97.5% of the total pixels during training, watermark false negatives are highly favored. This results in image segmentation outputs that are very conservative in their prediction of watermark pixels, only predicting a small percentage as watermarks as shown in Figure 2.

Although the prediction generated by DeepLab is sufficient to identify the existence of a watermark in the image, it significantly reduces the accuracy of our watermark scoring step. In order to increase the accuracy, we propose a hybrid model as described in Section 3.3. For watermark scoring described in Section 3.4, we consider the size and location of the watermark, which requires an approximate segmentation of the image into watermark and non-watermark pixels.

Watermark Semantic Segmentation Models

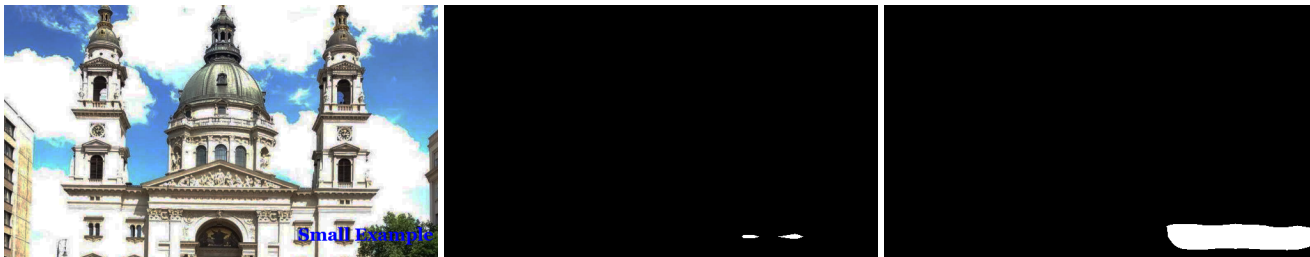


Figure 2: Semantic segmentation predictions for a small watermark in the corner of the image (*left*). This image demonstrates the hybrid model’s higher watermark pixel recall. Our strict image classification model’s low pixel recall results in the segmentation label (*middle*) with significantly fewer predicted watermark pixels than our hybrid model’s predicted segmentation label (*right*).

3.1. Semantic Image Segmentation

In order to generate a distraction score for watermarks, we must first detect watermark pixels. To achieve this, we train a model on images that contained watermarks. As a pre-processing step, images are scaled to be of uniform size. By eliminating negative examples and fixing the watermark class frequency, we reformulate the watermark scoring problem to a semantic segmentation one. This model is proficient in its segmentation of images into watermark and non-watermark pixels, allowing for accurate watermark scoring of images containing watermarks. However, as this model is trained on positive examples, this model alone has a higher false positive rate and lower image precision than our hybrid model, see Section 4.2 for details.

3.2. Image Classification

To address the high rate of false positives, we train a second, separate image classification model. This model is trained on a dataset of images that both do and do not contain watermarks and is meant to discriminate between the two. We modify the DeepLab architecture [7] by replacing the final Fully Connected CRF layer by likelihood thresholding. And we use a threshold of 0.75 to classify a pixel as containing a watermark. The resulting segmentation prediction is transformed into a binary mask by thresholding the number of predicted watermark pixels in the image. We set the threshold at a small fixed value based on the image size and observed noise in the segmentation label map.

3.3. Hybrid Model

Finally, we combine the two models described in Sections 3.1 and 3.2 by masking the predicted segmentation label from the image segmentation model with the binary image classification. This is equivalent to multiplying the pixel segmentation labels for the image I by w_I , where w_I is binary classification $\{0, 1\}$ for the image I .

$$L(i, j) = w_I \cdot S(i, j)$$

where $S(i, j)$ is the semantic segmentation prediction of image I at pixel (i, j) and $L(i, j)$ is the final segmentation label of the image for our hybrid model.

We designed this model to improve the accuracy of image comparison for images from a dataset with sparse positive examples. For each image, a final watermark distraction score is calculated as detailed in Sec. 3.4. We then define true positives for this image comparison as:

$$\sum_{y_i > y_j} \begin{cases} 1 & \text{if Score}(I_i) > \text{Score}(I_j) \\ 0 & \text{otherwise} \end{cases}$$

where for a pair of images, y_i is the true score of image I_i and y_j is the true score of image I_j . We seek to maximize the number of image pairs that we score correctly. That is, predicting a higher score for the image with more visually distracting watermarks. For a scoring function where we compute the normalized area of watermarked pixels, this is equivalent to maximizing the Intersection over Union (IOU), as defined in Section 4.2, of images that contain watermarks, while minimizing the number of incorrectly classified images. This reformulation of our problem motivates our hybrid model design, since for a segmentation label L_i of image I_i :

$$\max IOU(L_i), \quad I_i \in PositiveExamples$$

will be maximized for a model with the highest pixel IOU value on images containing watermarks. In the design of our semantic segmentation model, the pixel IOU was maximized. In addition, minimizing the number of image False Positives (iFP) and image False Negatives (iFN), as defined in Section 4.2, of our model is equivalent to maximizing:

$$\frac{iTP}{iTP + iFP + iFN}, \quad I \in BalancedDataset$$

where *BalancedDataset* is a dataset containing both watermarked and non-watermarked images. For a dataset

where $PositiveExamples \ll NegativeExamples$, we can assume $iFN \ll iFP$. Therefore, we can approximate this expression with:

$$\frac{iTP}{iTP + iFP}, I \in SparseDataset$$

This expression is the image precision of our dataset, which our image classification model maximizes. By design, our hybrid model obtains a higher precision than the image segmentation model, as its iFP is upper bound by the iFP of the image classification model. In addition, for images that are not iFN of the image classification model, the pixel recall is determined by the semantic segmentation model, which has a high pixel recall, as shown for an example in Figure 2. As a result, by combining the image classification and semantic segmentation models, we maximize the accuracy of our scoring function in the context of image comparison. A diagram of our proposed hybrid model is shown in Figure 1.

3.4. Watermark Distraction Scoring

Finally, we score images based on the total area and locations of their detected watermarks to represent their perceptual impact with a single score. This scoring function maps segmentation labels into a score in the range of $[0, 1]$, where images with a score of 0 do not contain watermarks and images with a score of 1 contain watermarks that are very distracting and visually obstructive. We characterize the weight of the watermark’s location as an isotropic 2D Gaussian function centered at the center of the image. We incorporate the total area of image I ’s watermarks into our image score by computing the weighted sum of the segmentation labels $L(i, j)$ with the Gaussian weights $g(i, j)$ as follows:

$$G(\sigma, L) = \sum_{i,j \in L} g(i, j)L(i, j)$$

We also assume that users’ scoring of image quality is not necessarily linear with respect to this weighted sum. We therefore fit the output to the user responses with a sigmoid function as:

$$Score(I) = \frac{1}{1 + e^{-\lambda(G(\sigma, L) - \alpha)}}$$

where α is the bias, σ is the standard deviation of the Gaussian and λ is the steepness of the sigmoid function. $G(\sigma, L)$ is the weighted sum of elements (i, j) in L with the value of the Gaussian at (i, j) . We optimize for α , σ , and λ by minimizing a Mean Squared Error:

$$\operatorname{argmin}_{\lambda, \sigma, \alpha} MSE\left(\frac{1}{1 + e^{-\lambda(G(\sigma, L) - \alpha)}}, y\right)$$



Figure 3: Example of an annotated image used as a segmentation label. Watermarks on the top right and left corners of the image are annotated with two polygons with an arbitrary numbers of vertices.

where y is the watermark score obtained from user responses. To fit our scoring function, we obtained a ground-truth dataset of 10k segmentation labels with corresponding watermark scores. Scores were obtained by displaying watermarked images and asking reviewers to give them a discrete score between $[0, 3]$ based on the size, locations, and obstructiveness of their watermarks with 0 being no watermark and 3 being a large and very obtrusive watermark.

4. Experiments

4.1. Datasets

We collected a proprietary dataset of 200k annotated images. Of these images, 62.5% contain watermarks. For images containing watermarks, the watermark pixel frequency is 6.011%. We randomly split our labelled data into three sets: training (80%), evaluation (10%), and validation (10%). We train our model on 160k annotated images. During training, we evaluate our model on an evaluation set of 20k images. And after training, we evaluate our model on a validation set of 20k images.

The images in our dataset are annotated as shown in Figure 3. Annotators are asked to draw polygons around each watermark region in the image, which are then converted into a binary segmentation label. If an image contains no watermark annotators are instructed to add no labels and we interpret the result accordingly.

4.2. Evaluation Metrics

We consider both pixel level and image level metrics when evaluating our model.

Pixel Metrics. We define pixel precision, recall and IOU as:

$$\begin{aligned} Precision &= \frac{TP}{TP + FP} \\ Recall &= \frac{TP}{TP + FN} \\ IOU &= \frac{TP}{TP + FP + FN} \end{aligned}$$

Dataset	mIOU
Watermarked (ours)	76.16
Balanced Watermarked (ours)	63.04
PASCAL VOC 2012 val	77.69
PASCAL-Context dataset	45.7
PASCAL-Person-Part	63.10
Cityscapes dataset	70.4

Table 1: Comparison of the mean IOU for our watermark datasets to the datasets in Chen et al. [7] for DeepLab model.

where a True Positive (TP) is a pixel that is correctly classified as a watermark pixel and a False Positive (FP) is a pixel that is incorrectly classified as a watermark pixel.

Image Metrics. We define image precision and recall as:

$$iPrecision = \frac{iTP}{iTP + iFP}$$

$$iRecall = \frac{iTP}{iTP + iFN}$$

where an image True Positive (iTP) is an image that is correctly predicted to contain a watermark.

Estimated Image Precision. In this paper, we assume that watermarked images comprise approximately 10% of our entire database based on a small subset of our entire database. Although our hybrid model’s image recall is lower than the segmentation model, it provides significant improvement in $iPrecision$ for datasets with sparse positive examples. We compute the estimated image precision ($ePrecision$) of our model for datasets with different percentages of positive examples as:

$$ePrecision = \frac{\beta iTP}{\beta iTP + (1 - \beta)iFP}$$

where β is the true fraction of watermarked images in our dataset, and iTP and iFP are computed from a balanced dataset of 50% watermarked images. If we compute $ePrecision$ with $\beta = 0.1$ for the semantic segmentation model shown in Table 4, only 26.13% of detected images would actually contain watermarks. On the other hand for the strict hybrid model, 79.51% of detected images would contain watermarks. This improvement increases the $ePrecision$ of our model, as the majority of images with a non-zero watermark scores are true positives. We compare $ePrecision$ values for our hybrid model to the image segmentation model in Section 4.4.

Mean IOU Comparison. For our image segmentation model, we obtain a mean IOU of 76% on our validation, similar to [7], as shown in Table 1. This mean IOU metric demonstrates the accuracy and precision of our watermark

Model	Precision	Recall	IOU
Semantic Segmentation	82.05	75.68	64.93
Image Classifier	95.42	43.04	42.17
Hybrid Classifier	83.29	69.60	61.07

Table 2: Pixel precision, recall and IOU for dataset with only watermarked images.

Model	Precision	Recall	IOU
Semantic Segmentation	68.97	75.68	56.46
Image Classifier	94.58	43.04	42.00
Hybrid Classifier	81.10	69.60	59.80

Table 3: Pixel precision, recall and IOU for dataset with 62.5% watermarked images. Our hybrid classifier has improvement over semantic segmentation model in pixel precision.

scoring function. For our image classification model, our mean IOU is lower because we trade pixel recall for image precision. If we weight our mean IOU to balance the frequency of the watermark and non-watermark classes, where watermark pixels make up 6% of image pixels (as detailed in Sec. 4.1), our mean IOU is 63.04%.

The lower value demonstrates the difficulty of the watermark problem, as watermarks vary significantly in shape, pattern and transparency. Moreover we would also like to note that mean IOU is not very high because of the fact that most of the annotated images have background pixels included in the labels such as in Figure 3.

4.3. Semantic Segmentation Evaluation

We train our semantic segmentation model on 160k watermarked images, as detailed in Sec. 4.1. The results are shown in Table 2. This model attains a high pixel precision and recall, with an IOU of 65, comparable to the mean IOU values reported in [7]. However, when we add negative examples to the validation set, the pixel precision decreases to 69%, with an image precision of only 76%. For images with watermarks, this model proficiently segments the images into watermark and non-watermark regions. However, this model is unable to effectively filter non-watermarked images, as shown in Table 3. Our image classifier maintains a 95% pixel precision after we include negative examples in our validation set. In order to obtain this high precision, its watermark recall is only 43%. For our hybrid model, since the image false positives are upper bound by the image false positives of our image classifier, it maintains an image precision of 97%, as shown in Table 4. In addition, it attains a pixel recall of 70% and pixel precision of 83%.

4.4. Semantic Segmentation with a Balanced Set

As an alternative approach to our hybrid model, we train our semantic segmentation model with negative examples to obtain similar per pixel metrics to our hybrid model. A comparison of these metrics are shown in Table 5. For our

Model	iPrecision	iRecall	ePrecision
Semantic Segmentation	76.10	97.20	26.13
Image Classifier	97.16	84.63	79.51
Hybrid Classifier	97.21	84.61	79.51

Table 4: Image precision and recall for a dataset with 62.5% watermarked images, weighted by image class frequency. We show our estimated image Precision (ePrecision) for a dataset with 10% watermarked images as well. Our hybrid classifier maintains the precision of our image classifier.

Model	Precision	Recall	IOU
Semantic Segmentation	85.62	67.99	61.03
Hybrid Classifier	83.29	69.60	61.07

Table 5: Pixel precision, recall and IOU for watermarked images.

Model	iPrecision	iFP	ePrecision
Semantic Segmentation	94.24	471	64.51
Hybrid Classifier	97.21	201	79.51

Table 6: Image precision and number of image False Positives with 62.5% watermarked images, and estimated image Precision with 10% watermarked images.

hybrid classifier, we match per pixel metrics obtained with semantic segmentation. In a balanced validation set, the image precisions of these two models are comparable. Our semantic segmentation model obtains 94.24% image precision with a balanced validation set, only a 3% decrease in precision from our hybrid model with 97.21% precision.

However, when we consider our true dataset, our hybrid model significantly outperforms the semantic segmentation model. The semantic segmentation model has over double the false positives as our hybrid model, with 471 *iFP* as opposed to only 201 *iFP* in our hybrid model. In a dataset with sparse positive examples, this increase in false positives has a large effect on the image precision. For our true dataset with 10% watermarked images, only 65% of detected images would contain watermarks. The estimated image precision of our hybrid model is higher, with 80% of detected images containing watermarks, as shown in Table 6.

4.5. Text Detectors

We evaluate our validation set on Google Cloud API’s text detector [2]. This text detector is an OCR (optical character recognition) system for extracting text from images. We consider a text detector as an alternative for detecting watermarks, as they commonly contain text. However, we identify two limitations to using a text detector for general watermark detection. Firstly, text in watermarks only comprises a subset of watermark pixels, resulting in a low per pixel recall as shown in Table 7. Secondly, non-watermark text in images increases the false positive rate. We observe a high false positive rate for non-watermark text on billboards, menus, signs, and fliers. Figure 4 shows examples of the text detector’s false positives that our hybrid model correctly predicts to not contain watermarks.

Model	Precision	Recall	IOU	iPrecision	iRecall
Text Detector	33.08	15.35	11.71	65.91	61.89
Hybrid	81.10	69.60	59.80	97.21	84.61

Table 7: Comparison of precision and recall metrics for text and hybrid classifiers.



Figure 4: Google Cloud API’s text detector [2] falsely predicts images to contain watermarks. Our hybrid model predicts these images to not contain watermarks.

4.6. Results on Images From a Different Domain

We also run our algorithm on publicly available images containing watermarks on Flickr [1]. Table 11 shows the original images, detected watermarks, and their final watermark scores. The results show the ability of our model to detect various kinds of watermarks including text (even when rotated), logos, and transparent and solid watermarks. Also, the estimated watermark scores are highly correlated with the watermarks’ perceptual impact on the images, such as when the watermark is covering most of the image, in which case our model labels the result with the highest watermark score of 1. When the watermark is small and on the edge of the image our model labels the image with a watermark score near zero. Please see the supplementary material for more results.

5. Watermark Scoring Evaluation

We collected 10k images for our watermark scoring dataset by displaying images to users and asking them to score them based on the size and location of the watermarks in each image. They were given four annotation options numbered 0 through 3, with 0 being an image with no watermarks, 1 being an image with small watermarks near its edges and 3 being an image with large, central watermarks. We split our dataset into a training set of 8k to fit our scoring function and a validation set of 2k to compute the MSE of the function, which is 0.041 for normalized score values in the range [0, 1]. We use the ground truth segmentation labels L_i for each image as the input to our scoring function as defined in Section 3.4.

The optimal σ value of our Gaussian weight function is found to be 0.44. Figure 5 visualizes the Gaussian with this sigma value on the fixed image size of our dataset. Weighting the pixel labels with this sigma value gives wa-

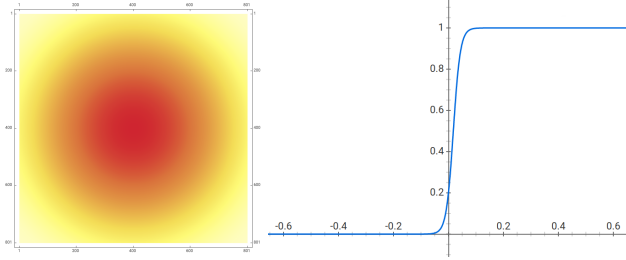


Figure 5: Visualization of the isometric 2D Gaussian (left) and the sigmoid function (right) used in our watermark scoring function by fitting them on human evaluations of watermarked images.

termark pixels in the center of the image a considerably larger weight than edge watermarks, with pixels near the corners scaled by a small weight.

The optimal λ value of our sigmoid function is found to be 78, which results in a very steep sigmoid function, as shown in Figure 5, that is close to a step function. This optimal value models the human response to an increase in the area of the watermark in an image. If a watermark takes up more than a small portion of the image, it is given a high watermark score. For more central watermarks, the area percentage required for a score of "very distracting" is even lower.

With the final goal of using these watermark scores to downrank images that have obtrusive watermarks, we design an evaluation based on pairwise watermark score comparisons. We asked users to score 10k images by the visual impact of their watermarks. These scores were obtained by displaying an image to users and asking them to score the image based on how perceptually distracting the image's watermarks are. They were given a range of responses from $[0, 3]$, where 0 was reserved for images that did not contain watermarks and 3 was for images with very distracting watermarks. Each image was displayed to three users, and their responses are averaged to obtain the image's final score. This score represents how large of an effect the image's watermarks had on the image's perceptual quality. To evaluate our model's image ranking against the ground truth, we compute the accuracy of our ranking for all potential image pairs. In Table 8, we show the percentage of image pairs (A, B) with true ranking $A > B$, whose predicted score $\hat{A} > \hat{B}$. For instance, when all the images with score of 3 are compared against all the images with score of 1, in 95.36% of those pairs images with ground truth score of 3 have higher watermark score predicted by our model. In other words, our evaluation determines that for a quality ranking task our model will rank images with very distracting watermarks lower than images with ignorable watermarks 95% of the time.

In Table 9, we use the predicted segmentation labels from our hybrid model as input to our sigmoid function. In this experiment, we eliminate images that we predict to

	3	2	1
0	96.71	96.45	92.08
1	95.36	81.05	N/A
2	88.25	N/A	N/A

Table 8: Percentage pairwise accuracy for image pairs with different ground truth scores shown in the first row and the column. Evaluated on 10k images.

	3	2	1
0	N/A	N/A	N/A
1	96.14	78.39	N/A
2	87.80	N/A	N/A

Table 9: Percentage pairwise accuracy for image pairs with different ground truth scores shown in the first row and the column. Evaluated on 1k randomly sampled images from the validation set, with negative predictions removed.

	3	2	1
0	86.76	81.10	57.95
1	86.40	72.42	N/A
2	79.47	N/A	N/A

Table 10: Percentage pairwise accuracy for image pairs with different ground truth scores shown in the first row and the column. Evaluated on 1.7k randomly sampled images from the validation set.

not contain watermarks, as these images are not given a watermark score. Our model's ranking of images with very distracting watermarks against images with ignorable watermarks had an accuracy of 96%. In addition, our ranking accuracy of image pairs for all validation images is shown in Table 10.

6. Discussion and Future Work

We proposed a model to detect watermarks on images that generalizes to real world datasets, without any synthetic data. We consider our image scoring problem in the context of sparse positive examples with high variance. Previous work has produced interesting results for watermark detection, but these cases have been limited primarily to synthetic data with an evaluation set of select watermarks that were used to train the model. In our work, we focus on inferring a score for watermarked images that is accurate in the context of large-scale image ranking, which requires a generalized model that can recognize watermarks not present in our training set.

A potential future direction for watermark scoring is implementing a multi-class model. For this model, watermark pixels in images would be labelled based on their opacity in the image. This information could then be used in our scoring function to scale the weight of the predicted watermark pixels. Through our evaluation of our scoring function, a high accuracy can still be attained by only considering the segmentation of images into watermark and non-watermark regions.






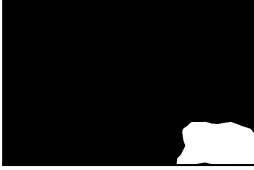



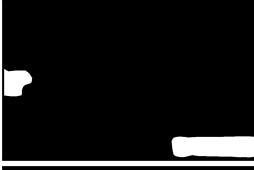
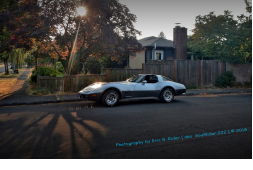


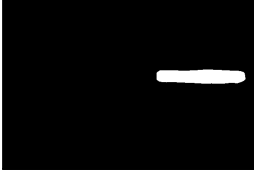






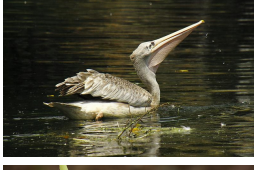

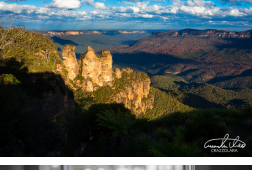

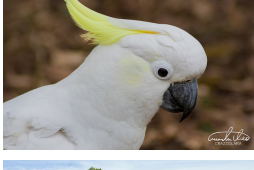



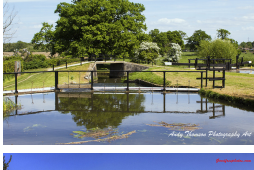

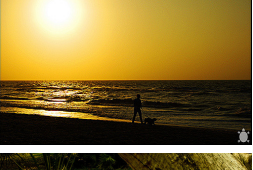


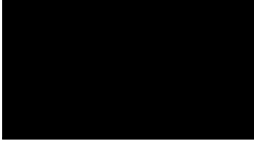

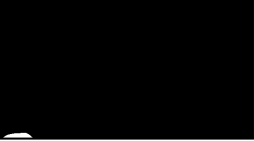


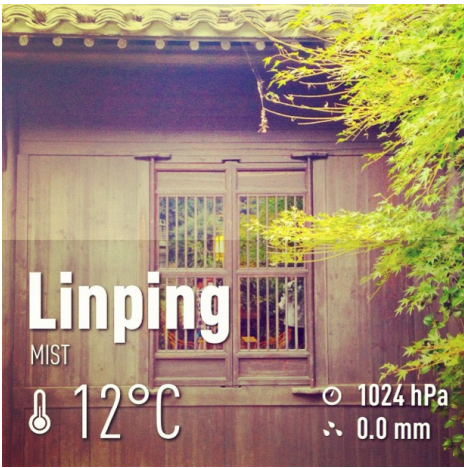
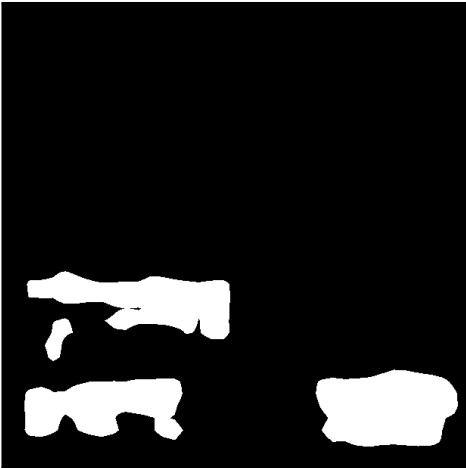


Original Image	Segmentation	Score	Original Image	Segmentation	Score
		1.0			0.998
		0.961			0.840
		0.831			0.641
		0.553			0.451
		0.379			0.370
		0.333			0.328
		0.292			0.266
		0.257			0.102
		0.093			0.033


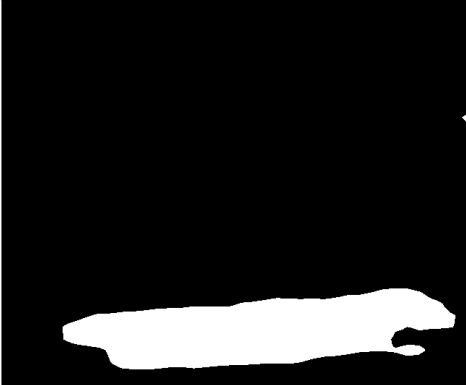

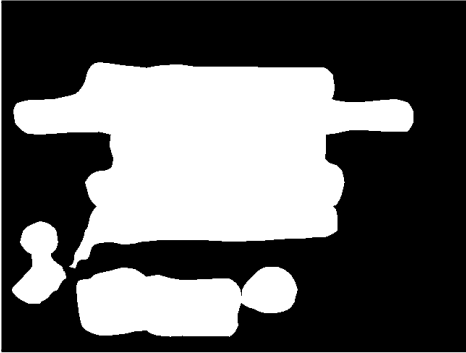

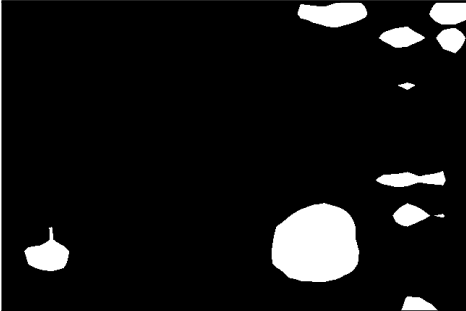

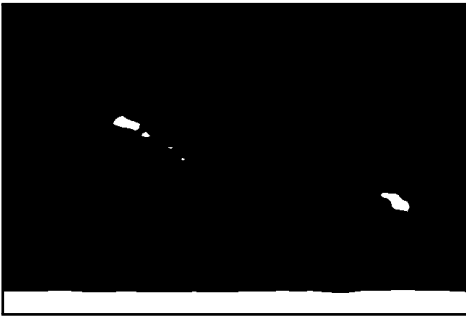



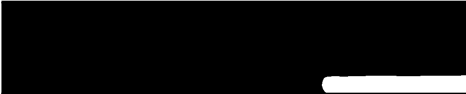
Table 11: Watermark detection results on Flickr images [1] that were not included in either training or testing. From left to right: original image, detected watermark segmentation, and final watermark score between [0, 1]. Please note that some watermarks are subtle to see in a printout, refer to the supplemental material for higher resolution.



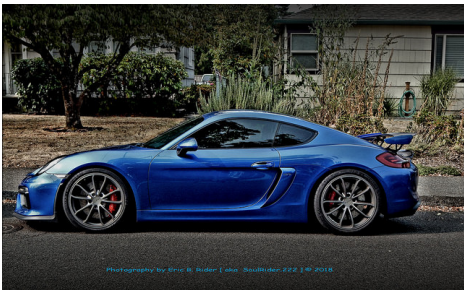


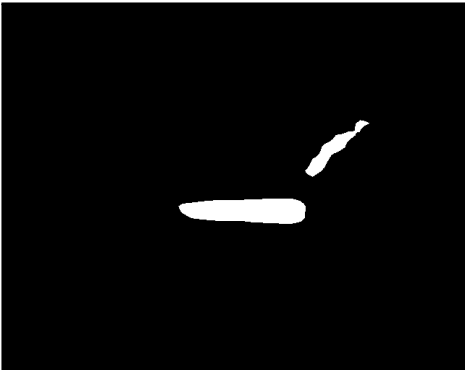



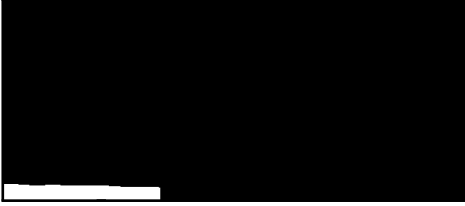
References


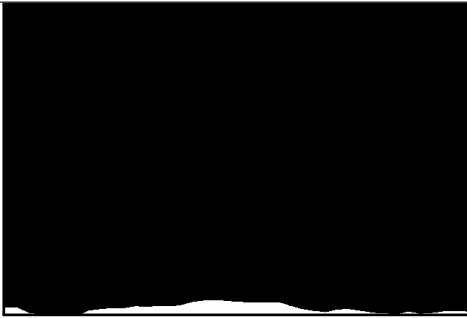

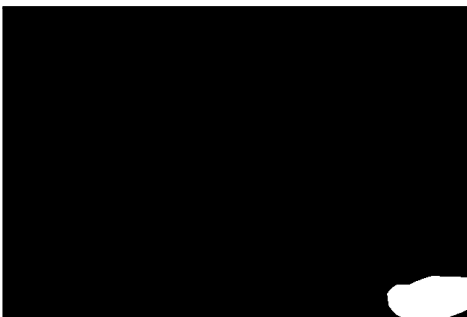

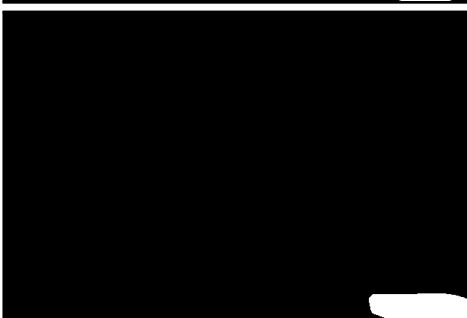


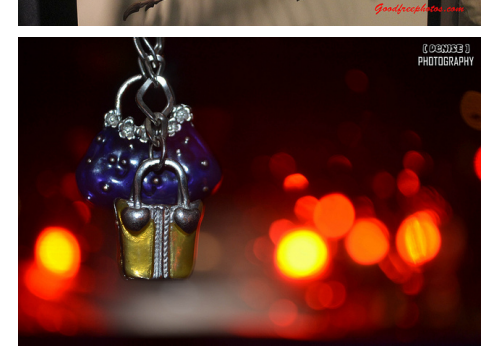

- [1] Flickr. <http://www.flickr.com>. 6, 8, 10
- [2] Google cloud api text detector. <https://cloud.google.com/vision/docs/detecting-text>. 1, 6
- [3] M. Belmont. Fully convolutional watermark removal attack. <https://github.com/marcbelmont/cnn-watermark-removal/>, 2018. 2
- [4] M. Bertalmio, G. Sapiro, V. Caselles, and C. Ballester. Image inpainting. In *Proceedings of the 27th annual conference on Computer graphics and interactive techniques*, pages 417–424, 2000. 2
- [5] G. W. Braudaway, K. A. Magerlein, and F. C. Mintzer. Protecting publicly available images with a visible image watermark. In *Electronic Imaging: Science & Technology*, page 126133, 1996. 2
- [6] L. Chen, G. Papandreou, I. Kokkinos, K. Murphy, and A. L. Yuille. Semantic image segmentation with deep convolutional nets and fully connected crfs. *CoRR*, abs/1412.7062, 2014. 1
- [7] L. Chen, G. Papandreou, I. Kokkinos, K. Murphy, and A. L. Yuille. Deeplab: Semantic image segmentation with deep convolutional nets, atrous convolution, and fully connected crfs. *CoRR*, abs/1606.00915, 2016. 1, 2, 3, 5
- [8] L. Chen, G. Papandreou, F. Schroff, and H. Adam. Rethinking atrous convolution for semantic image segmentation. *CoRR*, abs/1706.05587, 2017. 1
- [9] L. Chen, Y. Zhu, G. Papandreou, F. Schroff, and H. Adam. Encoder-decoder with atrous separable convolution for semantic image segmentation. *CoRR*, abs/1802.02611, 2018. 1
- [10] J. Dai, K. He, and J. Sun. Instance-aware semantic segmentation via multi-task network cascades. *CoRR*, abs/1512.04412, 2015. 2
- [11] M. Dashti, R. Safabakhsh, M. Pourfard, and M. Abdollahifard. Video logo removal using iterative subsequent matching. In *AISP*, 2015. 2
- [12] T. Dekel, M. Rubinstein, C. Liu, and W. T. Freeman. On the effectiveness of visible watermarks. In *2017 IEEE Conference on Computer Vision and Pattern Recognition (CVPR)*, pages 6864–6872, July 2017. 1
- [13] K. He, G. Gkioxari, P. Dollár, and R. B. Girshick. Mask R-CNN. *CoRR*, abs/1703.06870, 2017. 2
- [14] C.-H. Huang and J.-L. Wu. Attacking visible watermarking schemes. In *Multimedia, IEEE Transactions*, pages 16–30, 2004. 2
- [15] M. S. Kankanhalli and K. Ramakrishnan. Adaptive visible watermarking of images. In *Multimedia Computing and Systems, 1999. IEEE International Conference on*, volume 1, pages 568–573, 1999. 2
- [16] A. Levin, D. Lischinski, and Y. Weiss. Protecting publicly available images with a visible image watermark. In *A closed-form solution to natural image matting. Pattern Analysis and Machine Intelligence*, pages 228–242, 2008. 1
- [17] S.-C. Pei and Y.-C. Zeng. A novel image recovery algorithm for visible watermarked images. In *Information Forensics and Security, IEEE Transactions*, pages 543–550, 2016. 2
- [18] P. H. O. Pinheiro, R. Collobert, and P. Dollár. Learning to segment object candidates. *CoRR*, abs/1506.06204, 2015. 2
- [19] P. H. O. Pinheiro, T. Lin, R. Collobert, and P. Dollár. Learning to refine object segments. *CoRR*, abs/1603.08695, 2016. 2
- [20] J. Wang and M. F. Cohen. Image and video matting: a survey. In *Now Publishers Inc*, 2008. 1
- [21] J. Wang, Q. Liu, H. L. L. Duan, and C. Xu. Automatic tv logo detection, tracking and removal in broadcast video. In *ICMM*, 2007. 2
- [22] W.-Q. Yan, J. Wang, and M. S. Kankanhalli. Automatic video logo detection and removal. In *Multimedia Systems*, 2005. 2


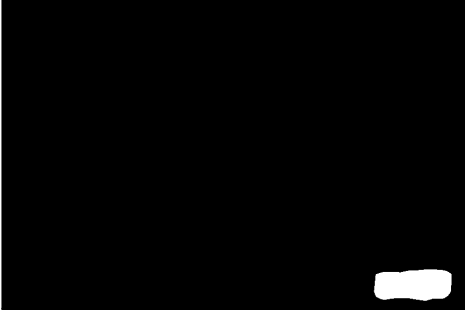





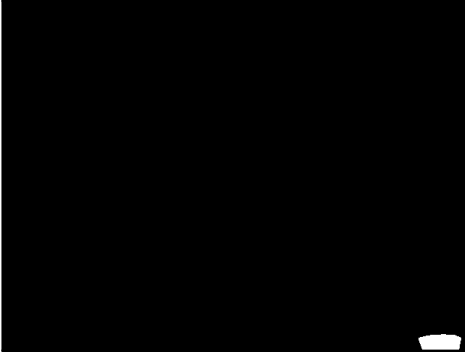

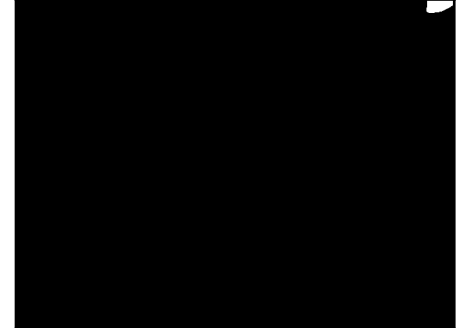
Table 12: More watermark detection results on Flickr images [1] that were not included in training or testing. From left to right: original image, detected watermark segmentation, and final watermark score between [0, 1]. Images are ordered by decreasing watermark scores.

Original Image	Segmentation	Watermark Score
		1.0
		1.0
		1.0

Original Image	Segmentation	Watermark Score
 <p>Portumna Marathon/Ultras 2011 - www.flickr.com/peterm7</p>		1.0
 <p>i'm a douchebag so i put huge annoying watermark on my cat photo so nobody can steal my beautiful photo © tm ®</p>		1.0
		0.989
 <p>Copones Restaurant & Live Music offers its guests the "Total Dining Experience" CoponesRestaurant.net photos by RicksonGarcia.com</p>		0.980
 <p>DoubleTake</p>		0.883
 <p>Serrasclimb Imagedesign ©2008</p>		0.877

Original Image	Segmentation	Watermark Score
 <p>Videographic & Photographer by Sam L. © 2015 London Picture Capital Agency http://londonpicturecapital.weebly.com/</p>		0.694
 <p>Photography by Steve B. Miller Editor: Steve Miller 1/10/2018</p>		0.536
 <p>Sarah Robertson</p>		0.533
 <p>Maggie Deegan Photography</p>		0.478
 <p>Maggie Deegan Photography</p>		0.474

Original Image	Segmentation	Watermark Score
 <p>SARAH RAE IMAGES</p>		0.356
 <p>CRAZZOLARA</p>		0.330
 <p>Denise Mattos</p>		0.308
 <p>Good4u.com</p>		0.204
 <p>PHOTOGRAPHY</p>		0.206

Original Image	Segmentation	Watermark Score
		0.195
		0.178
		0.101
		0.045
		0.023